2014

Central memory CD8+ T lymphocytes mediate lung allograft acceptance

Alexander Sasha Krupnick
Washington University School of Medicine in St. Louis

Xue Lin
Washington University School of Medicine in St. Louis

Wenjun Li
Washington University School of Medicine in St. Louis

Ryuiji Higashikubo
Washington University School of Medicine in St. Louis

Bernd H. Zinselmeyer
Washington University School of Medicine in St. Louis

See next page for additional authors

 Related Commentary, page 967

Central memory CD8+ T lymphocytes mediate lung allograft acceptance

Alexander Sasha Krupnick,[1] Xue Lin,[1] Wenjun Li,[1] Ryuiji Higashikubo,[1] Bernd H. Zinselmeyer,[2] Hollyce Hartzler,[1] Kelsey Toth,[1] Jon H. Ritter,[3] Mikhail Y. Berezin,[4] Steven T. Wang,[4] Mark J. Miller,[5] Andrew E. Gelman,[1,2] and Daniel Kreisel[1,2]

[1]Department of Surgery and [2]Department of Pathology and Immunology, Washington University in St. Louis, St. Louis, Missouri, USA. [3]Department of Laboratory Medicine and Pathology, University of Minnesota, Minneapolis, Minnesota, USA. [4]Department of Radiology and [5]Department of Medicine, Washington University in St. Louis, St. Louis, Missouri, USA.

Memory T lymphocytes are commonly viewed as a major barrier for long-term survival of organ allografts and are thought to accelerate rejection responses due to their rapid infiltration into allografts, low threshold for activation, and ability to produce inflammatory mediators. Because memory T cells are usually associated with rejection, preclinical protocols have been developed to target this population in transplant recipients. Here, using a murine model, we found that costimulatory blockade–mediated lung allograft acceptance depended on the rapid infiltration of the graft by central memory CD8+ T cells (CD44^{hi}CD62L^{hi}CCR7+). Chemokine receptor signaling and alloantigen recognition were required for trafficking of these memory T cells to lung allografts. Intravital 2-photon imaging revealed that CCR7 expression on CD8+ T cells was critical for formation of stable synapses with antigen-presenting cells, resulting in IFN-γ production, which induced NO and downregulated alloimmune responses. Thus, we describe a critical role for CD8+ central memory T cells in lung allograft acceptance and highlight the need for tailored approaches for tolerance induction in the lung.

Introduction

While transplantation has become an accepted form of therapy for end-stage organ failure, formidable immunologic barriers limit long-term allograft survival. The currently accepted clinical immunosuppression protocols, consisting of life-long administration of calcineurin inhibitors, steroids, and antimetabolites, decrease immunosurveillance for both malignancies (1) and infectious diseases (2). Perioperative inhibition of lymphocyte activation through blockade of costimulatory pathways mediates acceptance of several types of allografts in murine models (3–5). Clinical data point to the efficacy of costimulatory blockade for the treatment of autoimmune diseases in humans (6, 7). Based on these data, costimulatory blockade is being actively evaluated in human solid organ transplantation (8). This would be very advantageous for lung transplantation, in which patients incur higher rates of graft loss compared with recipients of other solid organs (9) and suffer more infectious complications due to constant exposure of lung allografts to the external environment (10, 11).

Alloreactive memory T cells are generated through previous blood transfusions, pregnancy, or cross reactivity to viral or environmental antigens in a process known as heterologous immunity (12). When compared with naive T cells, memory T cells have lower activation requirements and can rapidly trigger alloimmune responses through the synthesis of multiple inflammatory cytokines and cytolytic effector molecules (12). Furthermore, this cell population is relatively resistant to immunosuppression, such as costimulatory blockade (13, 14). Multiple studies have established that early infiltration of CD8+ memory T cells into allografts, such as hearts, kidneys, and livers, facilitates accelerated rejection and presents a barrier to immunosuppression-mediated long-term graft survival (12, 15–19). Therefore, preclinical studies have focused on targeting this cell population in an effort to improve the survival of solid organ allografts, such as kidneys (17, 20, 21). However, some reports have indicated that CD8+ T cells with phenotypic and functional characteristics of memory cells can also downregulate immune responses. While it is well recognized that CD8+ memory T cells express CD122, the β subunit of the IL-2 receptor, recent work has shown that CD122+-expressing CD8+ T cells can have regulatory capacity (22). CD8+CD122+PD1+ T lymphocytes, for example, suppress T cell proliferation and production of inflammatory cytokines in an IL-10–dependent fashion (22). Another study showed that memory-like CD8+ T cells expressing the ectonucleotidase CD38 suppress CD4+ T cell activation in antigen-independent fashion in vitro and attenuate autoimmune responses in vivo (23). Immune regulation by these CD8+ T cells was dependent on production of IFN-γ and direct contact with the effector CD4+ T cells. Similarly, rapid bystander production of IFN-γ by memory CD8+CD44^{hi} CD62L^{hi} T cells has been shown to inhibit the development of Th2-driven allergic airway inflammation (24).

Here, we report that, in contrast to what has been described for other organ transplants, early infiltration of CD8+CD44^{hi} CD62L^{hi}CCR7+ central memory T cells is critical for lung allograft acceptance, due to IFN-γ–mediated induction of local NO. Our findings identify a novel mechanism of allograft acceptance that challenges the currently accepted paradigm of global T cell depletion as induction therapy for lung transplant recipients.

Results

Both CD4+ and CD8+ T lymphocytes can mediate lung allograft rejection. Lung allograft rejection is diagnosed and graded based on histological findings of cellular infiltrates (25). A wide variety of leukocytes, including B cells, macrophages, neutrophils, and natural killer cells, have been shown to contribute to rejection of solid organs (26–28), and to date it has not been established whether T lymphocytes are necessary to mediate lung allograft rejection. To

Conflict of interest: The authors have declared that no conflict of interest exists.
Citation for this article: *J Clin Invest.* 2014;124(3):1130–1143. doi:10.1172/JCI71359.

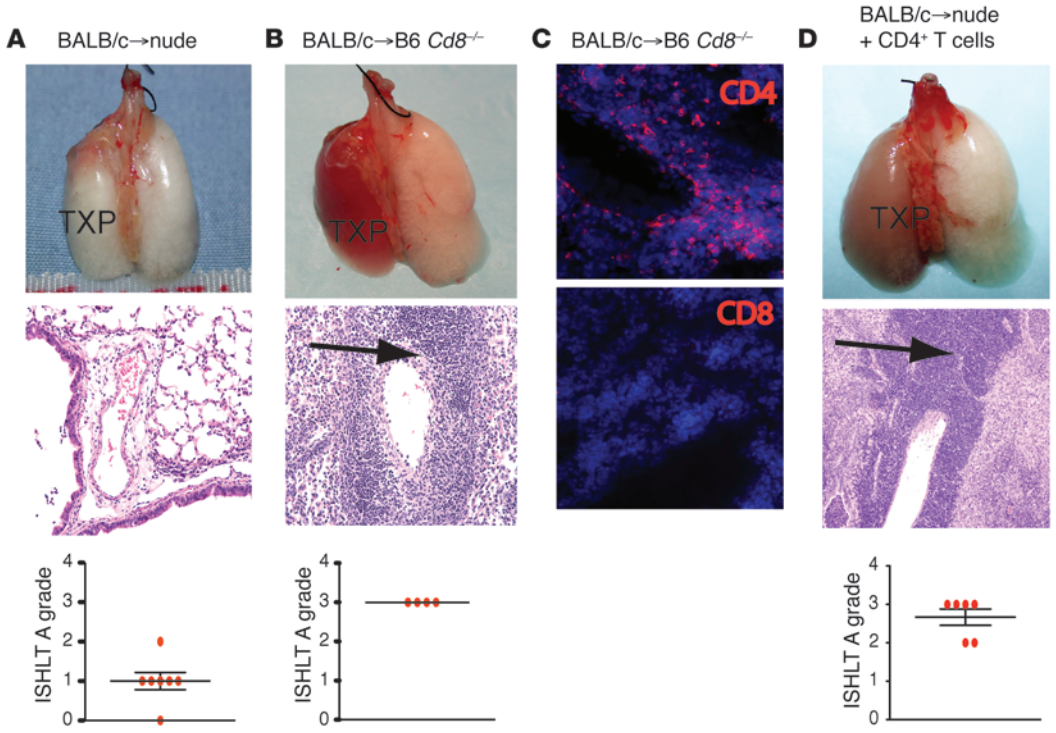

Figure 1
Cellular mechanisms of lung allograft rejection in the absence of immunosuppression. (**A**) BALB/c→nude lung grafts remain ventilated and free of inflammation, as demonstrated by gross appearance, histology, and ISHLT A grade. (**B**) BALB/c→B6 *Cd8*$^{-/-}$ lung grafts are rejected acutely within a week of transplantation, as evidenced by graft collapse due to loss of ventilation and by severe perivascular infiltration with inflammatory cells. (**C**) Perivascular infiltration in BALB/c→B6 *Cd8*$^{-/-}$ lung grafts was composed of CD4$^+$ but not CD8$^+$ cells. (**D**) Reconstitution of nude mice with B6 CD4$^+$ T cells results in rejection of transplanted BALB/c grafts (P = 0.0039 compared with **A** by Mantel-Haenszel χ^2 test). All gross and histological appearances as well as rejection grades represent grafts at 7 days after transplantation (original magnification, ×200 [histology, H&E staining and immunohistochemical staining]). TXP denotes graft, and arrows point to perivascular infiltrates.

address this issue, we transplanted BALB/c lungs into allogeneic athymic nude mice and determined that, in contrast to wild-type recipients (29), these grafts remain ventilated, with little inflammation 1 week after transplantation (Figure 1A) and long term (30). We have shown previously that, unlike the case for cardiac transplants, lung allografts can be rejected in the absence of CD4$^+$ T cells (31). To test whether CD8$^+$ T cells are essential for the rejection of pulmonary allografts, we transplanted BALB/c lungs into CD8$^+$ T cell–deficient B6 recipients (referred to herein as B6 *Cd8*$^{-/-}$ recipients) and noted histological changes of severe acute rejection with perivascular lymphocytic infiltrates comparable to those seen in CD8$^+$ T cell–sufficient B6 recipients (Figure 1B). Immunostaining of these grafts demonstrated extensive infiltration with CD4$^+$ T cells and no detectable CD8$^+$ T cells (Figure 1C). Furthermore, reconstitution of nude mice with CD4$^+$ T cells led to rejection of lung allografts by ISHLT A grade (32) (Figure 1D). Taken together with previously published data from our laboratory (31), we conclude that thymically derived T lymphocytes are necessary for lung allograft rejection and that either CD4$^+$ or CD8$^+$ T cells are sufficient to mediate this process.

CD8$^+$ T lymphocytes are critical for lung allograft acceptance. We have previously demonstrated that immunosuppression through blockade of the CD28/B7 and CD40/CD154 costimulatory pathways leads to long-term lung allograft acceptance in the BALB/c→B6 (31, 33) as well as other strain combinations (30). Regulatory CD4$^+$ T cells have been shown to play a critical role in costimulatory blockade–mediated acceptance of heart, skin, and islet allografts as well as amelioration of autoimmune diseases (4, 5, 34–38). However, recipient bulk CD4$^+$ T cell antibody-mediated depletion did not affect the fate of immunosuppressed lung allografts with rejection grades comparable to wild-type costimulatory blockade–treated hosts (Figure 2, A and B). While regulatory B cells have been described in some models of solid organ transplantation (39), we were still able to induce BALB/c lung allograft acceptance in B6 B cell–deficient mice (Supplemental Figure 1; supplemental material available online with this article; doi:10.1172/JCI71359DS1). Surprisingly, pulmonary allografts transplanted into costimulatory blockade–treated B6 CD8$^+$ T cell–depleted mice (Figure 2C) or B6 *Cd8*$^{-/-}$ mice (Figure 2D) were acutely rejected, with severe graft inflammation. The appearances of these grafts and rejection grades were similar to what we have reported previously for lungs transplanted into nonimmunosuppressed allogeneic recipients (40). Adoptive transfer of wild-type B6 CD8$^+$ T cells into immunosuppressed B6 *Cd8*$^{-/-}$ recipients restored acceptance of BALB/c lungs (Figure 2E). Seven days after engraftment, we observed an increase in CD4$^+$Foxp3$^+$ T cells in lung allografts of immunosuppressed BALB/c→B6 and BALB/c→B6 *Cd8*$^{-/-}$ recipients compared with lungs from untransplanted controls (Figure 3A). However, the proportion of CD4$^+$ T cells expressing Foxp3 in lung allografts was higher in the presence of CD8$^+$ T cells. No such differences were evident in spleens of

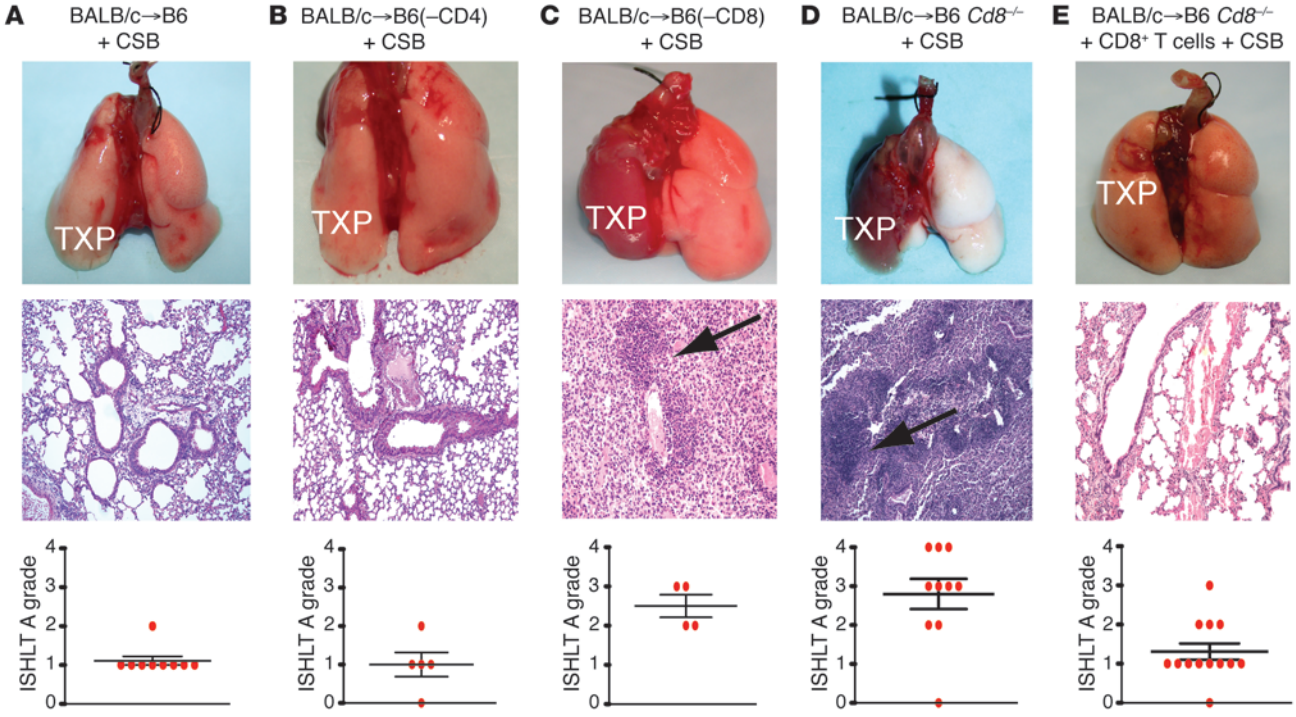

Figure 2
Cellular mechanisms of CSB-mediated lung acceptance. BALB/c lungs transplanted into (**A**) B6 or (**B**) CD4-depleted B6 recipients remain ventilated with minimal inflammation, with gross appearance, histology, and numerical ISHLT A rejection grade shown. Rejection grades were not significantly different (Mantel-Haenszel χ^2 test, $P = 0.500$). BALB/c lungs transplanted into (**C**) CD8-depleted or (**D**) *Cd8*$^{-/-}$ B6 recipients are rejected ($P < 0.002$ compared to **A** by Mantel-Haenszel χ^2 test). (**E**) Acceptance is restored in B6 *Cd8*$^{-/-}$ mice after CD8$^+$ T cell injection ($P = 0.613$ vs. **A** by Mantel-Haenszel χ^2 test). All gross and histological appearances as well as rejection grades represent grafts at 7 days after transplantation (original magnification, ×200 [histology, H&E staining]). TXP denotes graft, and arrows point to perivascular infiltrates.

transplanted mice (Supplemental Figure 2). Thus, CD8$^+$ T cells play a critical role in mediating lung allograft acceptance.

Based on the finding that CD4$^+$ T cells can trigger lung rejection in the absence of CD8$^+$ T cells, we next decided to evaluate CD4$^+$ T lymphocyte responses in the presence or absence of CD8$^+$ T cells. We injected CFSE-labeled congenic B6 CD45.1$^+$CD4$^+$ T cells into costimulatory blockade–treated B6 wild-type or B6 *Cd8*$^{-/-}$ recipient mice at the time of BALB/c lung transplantation and observed enhanced proliferation of this cell population in B6 *Cd8*$^{-/-}$ hosts compared with that in B6 wild-type hosts (Figure 3B). We found that, after transfer into B6 *Cd8*$^{-/-}$ recipients, several other costimulatory receptors, such as CD27, ICOS, and OX40, were upregulated on CD4$^+$ T cells compared with B6 wild-type hosts, while levels of CD28 and CD154 were comparable in these two groups (Figure 3B). We considered the possibility that costimulatory requirements of CD4$^+$ T lymphocytes may be altered in the absence of CD8$^+$ T cells and blockade of CD40/CD154 and CD28/B7 pathways may be insufficient to ameliorate CD4$^+$ T cell–mediated rejection (41). To address this, we inhibited CD27/CD70, ICOS/ICOS ligand, and OX40/OX40 ligand pathways in addition to blocking CD28/B7 and CD40/CD154 pathways in B6 *Cd8*$^{-/-}$ recipients of BALB/c lungs. However, this treatment regimen did not prevent lung allograft rejection when recipients lacked CD8$^+$ T cells (Figure 3C). These findings directly contrast with previous observations that depletion or deletion of CD8$^+$ T cells prolongs survival of skin and heart allografts when recipients are treated with costimulatory blockade (13, 37).

Accepting lung allografts are heavily infiltrated with central memory CD8$^+$CD44^{hi}CD62L^{hi}CCR7$^+$ T cells that can downregulate alloimmune responses. Costimulatory blockade has been described to mediate graft acceptance through the generation of regulatory T lymphocytes (4, 5, 34–38). In order to evaluate whether CD8$^+$ T lymphocytes with regulatory capacity develop in costimulatory blockade–treated lung recipients, we isolated CD8$^+$ T cells from the lung grafts and spleens of such mice and used them as "regulators" in in vitro mixed lymphocyte reactions (MLRs) (Figure 4A). We found that CD8$^+$ T lymphocytes isolated from accepting BALB/c→B6 lung allografts, but not spleens of these recipients, inhibited proliferation and blasting of B6 CD45.1$^+$CD4$^+$ (Figure 4B) and B6 CD45.1$^+$CD8$^+$ T lymphocytes (Figure 4C) when stimulated with BALB/c splenocytes. These findings suggested that CD8$^+$ T cells with regulatory capacity accumulate in accepting lung allografts. While described to have regulatory function in other models (42–44), very few CD8$^+$IL-10$^+$ or CD8$^+$Foxp3$^+$ cells were detectable in accepting lung allografts (Figure 5A). Notably, however, a large portion of CD8$^+$ T cells in accepting grafts had the capacity to produce IFN-γ and expressed phenotypic markers consistent with central memory T lymphocytes (CD44^{hi}CD62L^{hi}CCR7$^+$) (45). By contrast, most CD8$^+$ T cells in the spleens of graft-accepting recipients were naive (CD44^{lo}CD62L^{hi}), with lower levels of IFN-γ production (Figure 5B).

While the vast majority of studies suggest that memory T lymphocytes potentiate alloimmune responses and inhibit tolerance induction (46, 47), it is possible that certain subsets of these cells

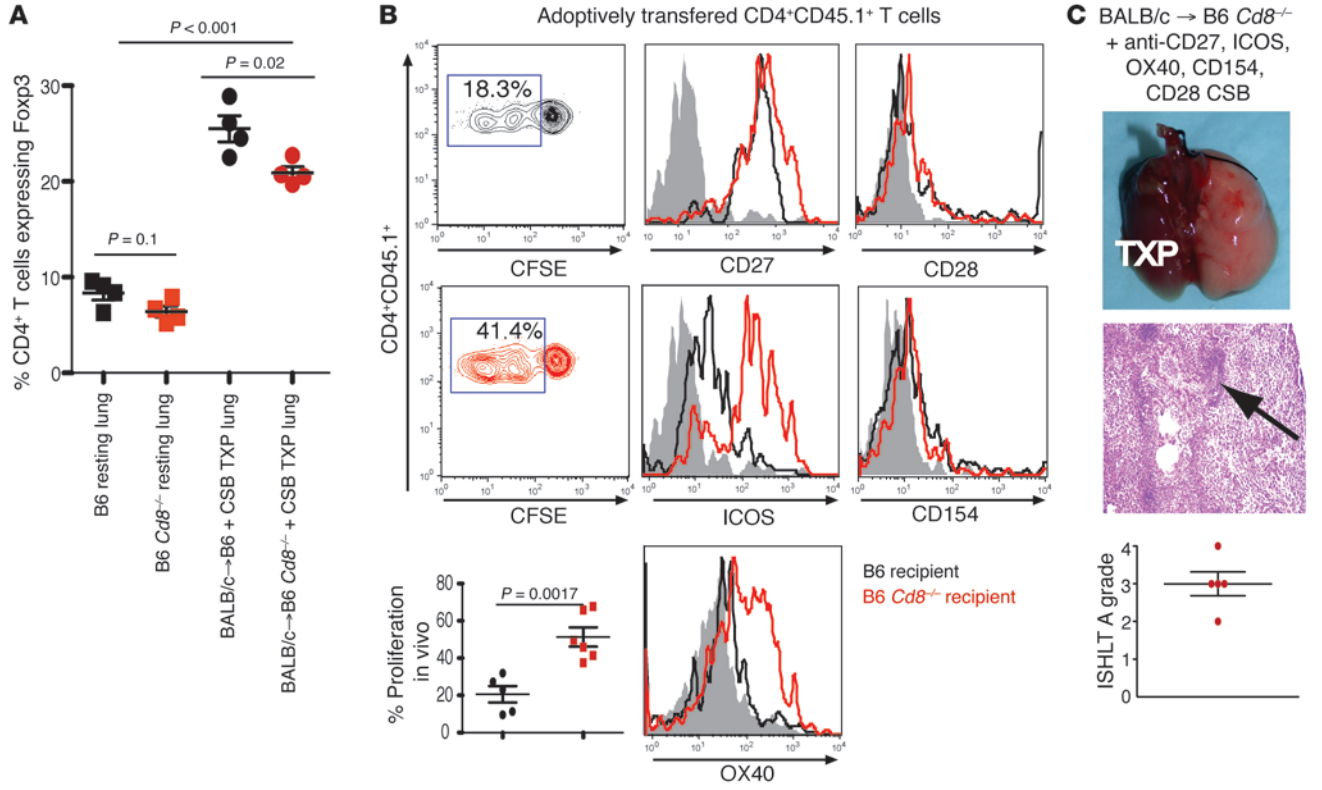

Figure 3

CD4+ T lymphocyte responses in CSB-treated lung transplant recipients. (**A**) The proportion of lung-resident CD4+Foxp3+ T cells is not different in resting B6 and B6 *Cd8*$^{-/-}$ lungs. These numbers do increase, however, after allograft transplantation, and a higher abundance of graft-infiltrating CD4+Foxp3+ T cells is detectable in B6 compared with B6 *Cd8*$^{-/-}$ lung graft recipients (comparison between resting and transplanted lungs by ANOVA and comparison between B6 and B6 *Cd8*$^{-/-}$ groups by unpaired *t* test). (**B**) Proliferation of B6 CD4+CD45.1+ T cells was greater after injection into B6 *Cd8*$^{-/-}$ (51.3% ± 5%) than B6 wild-type (20.6% ± 4%) recipients ($P = 0.0017$ by unpaired *t* test). Proliferating CD4+CD45.1+ T cells in B6 *Cd8*$^{-/-}$ recipients upregulated CD27, ICOS, and OX40 but not CD28 or CD154 compared with wild-type mice. Numbers in contour plots represent the percentages of adoptively transferred CD4+CD45.1+ T cells that have undergone proliferation (shaded gray, isotype controls; black lines, B6 wild-type; red lines, B6 *Cd8*$^{-/-}$ recipients). (**C**) Inhibiting CD27/CD70, ICOS/ICOS ligand, and OX40/OX40 ligand in addition to blocking CD40/CD154 and CD28/B7 does not prevent rejection in the absence of CD8+ T cells ($P = 0.00074$ vs. Figure 2A by Mantel-Haenszel χ^2 test). All gross and histological appearances as well as rejection grades represent grafts at 7 days after transplantation (original magnification, ×200 [histology, H&E staining]). TXP denotes graft, and the arrow points to perivascular infiltrates.

may suppress alloreactivity (48). It is noteworthy that CD8+ T lymphocytes, including memory CD8+ T cells, were present in the lung at baseline, even in the absence of acute inflammation or alloantigen stimulation (Figure 6A). This has been attributed to the lung's constant exposure to the environment and need to mount rapid responses to pathogens (49). We next set out to investigate whether memory CD8+ T cells from lungs of resting mice also had regulatory capacity. For this purpose, we flow cytometrically sorted CD8+CD44^{hi}CD62L^{hi} central memory and CD8+CD44^{hi}CD62L^{lo} effector memory T lymphocytes (45) from resting B6 mice and used them as regulators in in vitro MLRs, using methods similar to those described above (Figure 4A). Interestingly, even without prior in vitro stimulation, central memory CD8+ T lymphocytes could suppress proliferation of B6 CD45.1+CD4+ T cells stimulated with BALB/c splenocytes (Figure 6B), albeit to a lesser extent than those derived from transplanted grafts (Figure 4B). However, freshly isolated CD8+ effector memory T lymphocytes had no effect on B6 CD45.1+CD4+ T cell proliferation (Figure 6B). To further evaluate whether different subsets of memory T cells could influence the alloimmune response, we generated central memory or effector memory CD8+ T cells in vitro by culturing B6 splenocytes with irradiated BALB/c stimulators in the presence of IL-15 or IL-2, respectively, as previously described (50, 51). B6 *Cd8*$^{-/-}$ mice reconstituted with central memory CD8+ T cells accepted, while those reconstituted with effector memory CD8+ T cells rejected, BALB/c lung allografts after costimulatory blockade (Figure 6, C and D). Collectively, these data demonstrate that subtypes of memory CD8+ T cells can differentially influence the alloimmune response and that central memory CD8+ T cells play a critical role in lung allograft acceptance.

Central memory CD8+ T cells suppress alloimmune responses through IFN-γ–mediated production of NO. Since central memory T cells are known to be rapid producers of proinflammatory cytokines, we next examined whether CD8+ T lymphocytes mediate lung allograft acceptance through secretion of TNF-α or IFN-γ. BALB/c lungs were accepted by TNF-α–deficient B6 recipients or B6 *Cd8*$^{-/-}$ mice that were reconstituted with TNF-α–deficient B6 CD8+ T cells (data not shown). By contrast, allograft acceptance was abrogated if recipient mice were pretreated with IFN-γ–neutralizing antibody or *Ifng*$^{-/-}$ animals were used as hosts (Figure

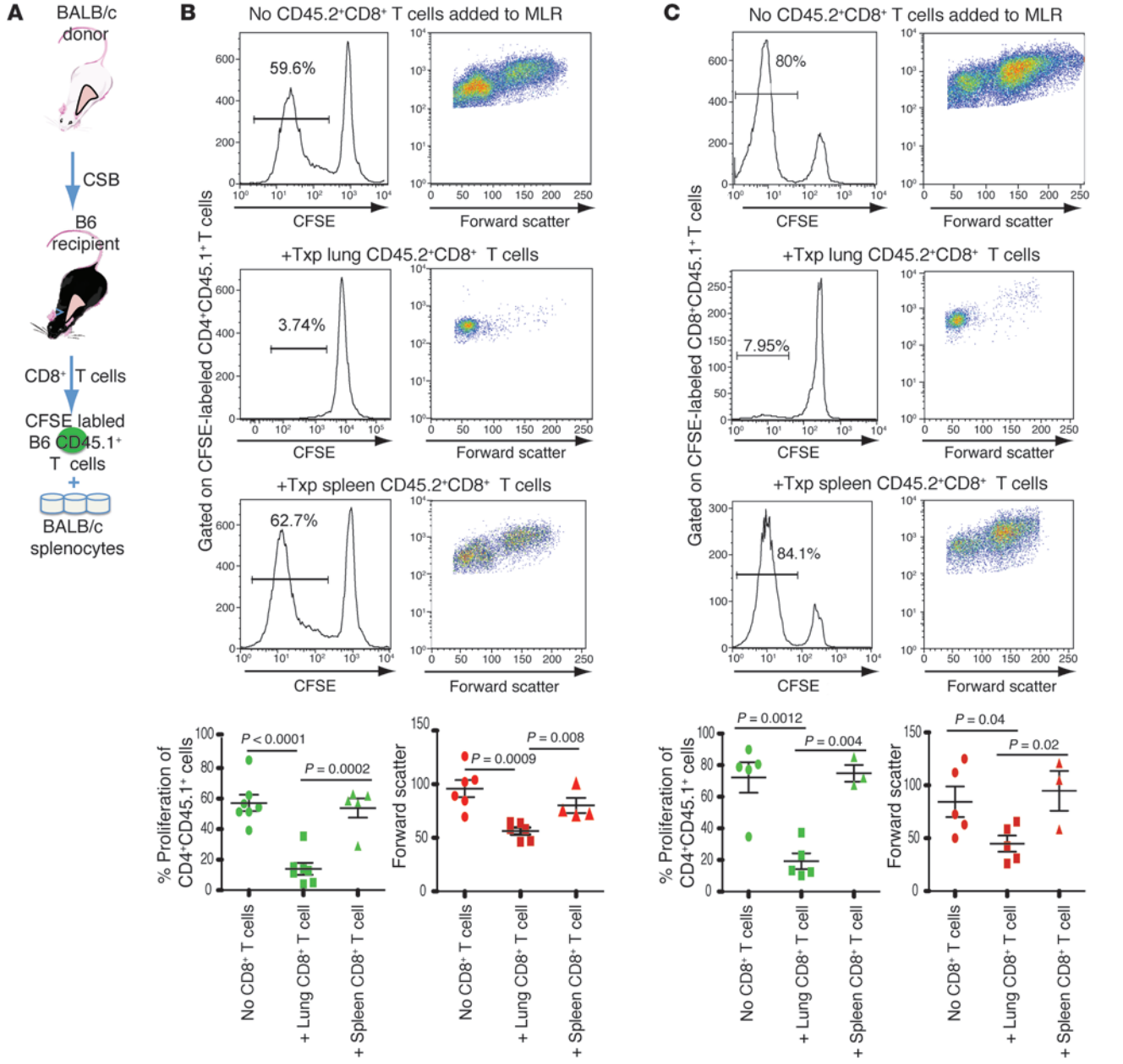

Figure 4

Graft-infiltrating CD8+ T cells play a critical role in downregulating alloimmune responses. (**A**) In vitro MLRs were established by isolating CD8+ T cells from CSB-treated BALB/c→B6 lung transplants and adding them as "regulators" to cocultures of BALB/c splenocytes (stimulators) and CFSE-labeled B6 CD45.1+ T cells (responders). (**B**) After 5 days of coculture the majority of (**B**) B6 CD4+CD45.1+ T cells or (**C**) B6 CD8+CD45.1+ T cells proliferate and blast, as evidenced by size (forward scatter) (top row). Proliferation and blasting is inhibited if CD8+ T cells isolated from accepting lung allografts are added to the MLRs (second row). No inhibition is evident if CD8+ T cells are isolated from the spleens of accepting mice (third row). Numbers in histograms represent percentages of (**B**) CD4+CD45.1+ or (**C**) CD8+CD45.1+ T cells that have undergone proliferation. Proliferation and size (forward scatter) in the respective groups are summarized in the bottom panels of **B** and **C**, with pair-wise comparison between groups performed by *t* test.

7A and Supplemental Figure 3). CD8+ T cell–mediated suppression of CD4+ T cell proliferation was also abrogated in vitro in the presence of IFN-γ–neutralizing antibody (Figure 7B). *Ifng* levels were significantly elevated in grafts after transplantation of BALB/c lungs into immunosuppressed B6 wild-type recipients compared with B6 *Cd8*$^{-/-}$ recipients (Figure 7C). Finally, injection of *Ifng*$^{-/-}$ CD8+ T cells into *Cd8*$^{-/-}$ mice failed to rescue BALB/c lung allografts from rejection, despite costimulatory blockade (Figure 7D). Taken together, these data demonstrate that IFN-γ production by CD8+ T cells plays a critical role in lung allograft acceptance.

In in vitro MLRs described above (Figure 4A), we noted that the majority of CD4+CD45.1+ responder T lymphocytes were not

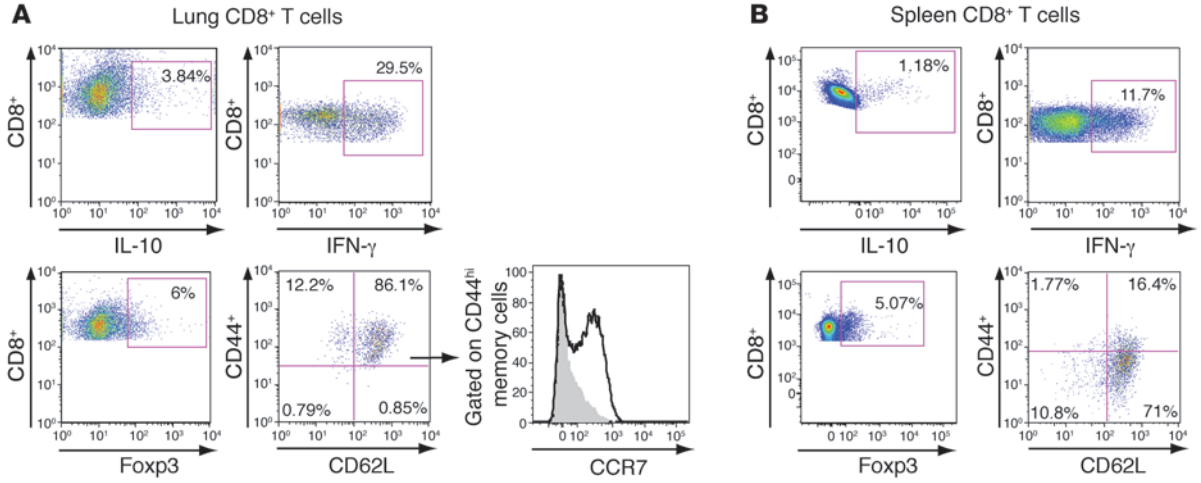

Figure 5

IFN-γ–producing central memory CD8⁺CD44^{hi}CD62L^{hi}CCR7⁺ T cells infiltrate accepting lung allografts. (**A**) Flow cytometry of CD8⁺ T lymphocytes in lung allografts of acceptors demonstrated few Foxp3⁺– or IL-10–producing cells. A large proportion of lung-resident CD8⁺ T cells had the capacity to produce IFN-γ and expressed a central memory phenotype (CD44^{hi}CD62L^{hi}CCR7⁺). (**B**) Fewer cells in spleens of lung graft recipients had the capacity to produce IFN-γ, and only few cells had a central memory T cell phenotype. Numbers in density plots in **A** and **B** represent percentages of CD8⁺ T cells expressing indicated markers. Phenotype of CD8⁺ T cells is representative of at least 4 separate experiments.

viable as measured by 7-AAD uptake when CD8⁺ T cells obtained from accepting lung allografts were added to the cultures (Figure 8A). Moreover, sensitivity of antigen-presenting cells to IFN-γ was critical for CD8⁺ T cell–mediated suppression, as proliferation of IFN-γ receptor–deficient CD4⁺ T cells was inhibited by allograft-derived CD8⁺ T cells, but no inhibition was evident if IFN-γ receptor–deficient antigen-presenting cells were used (Figure 8B). Also, CD8⁺ T cell–mediated suppression was not observed when T cells were activated with anti-CD3 and anti-CD28 antibodies in an antigen-presenting cell–free system (Figure 8C). Taken together, these data indicate that CD8⁺ T cells require antigen-presenting cells to downregulate T lymphocyte responses and the process depends on death of alloreactive cells.

Since metabolism of essential amino acids is a common mechanism of immunoregulation by antigen-presenting cells (52), we next added various pharmacologic inhibitors to in vitro MLRs and noted that only L-NNA (Nω-nitro-L-arginine), an inhibitor of endothelial, neuronal, and inducible NO synthase (eNOS, nNOS, and iNOS, respectively), and L-nil [N6-(1-iminoethyl)-L-lysine, dihydrochloride], a selective iNOS inhibitor, were able to attenuate CD8⁺ T cell–mediated suppression of CD4⁺ T lymphocyte proliferation (Figure 8D). Similarly, iNOS-deficient stimulators also prevented CD8⁺ T cell–mediated suppression of CD4⁺ T lymphocyte proliferation (Figure 8D). L-norvaline and 1-methyl-tryptophan (1-MT), selective inhibitors of arginase and indoleamine-pyrrole 2,3-dioxygenase (IDO), respectively, did not affect proliferation of CD4⁺ T cells. Furthermore, the addition of L-arginine did not reverse CD8⁺ T cell–mediated suppression, suggesting that amino acid depletion was not likely to be the principal method of immunoregulation (Figure 8D). This observation is consistent with the known role of IFN-γ in inducing iNOS expression (53).

Based on our finding that iNOS is critical to mediate suppression by CD8⁺ T cells and reports showing that local production of NO can downregulate immune responses by limiting proliferation and survival of T lymphocytes (54), we next set out to directly measure NO production in lungs. A near doubling in NO levels was evident in accepting BALB/c→B6 lung grafts compared with unmanipulated lungs of resting mice (Figure 8E). By contrast, we did not observe increases in NO levels in BALB/c→B6 *Cd8*$^{-/-}$ grafts. NO levels in the right native lungs of BALB/c→B6 and BALB/c→B6 *Cd8*$^{-/-}$ transplant recipients were comparable to resting lungs. To further examine the role of NO in graft acceptance, we next transplanted BALB/c lungs into costimulatory blockade–treated recipient B6 mice deficient in iNOS and observed that these grafts were rejected (Figure 8F). Thus, lung transplant acceptance is dependent on NO production by graft-infiltrating recipient cells.

Gα$_i$-coupled chemokine receptors regulate trafficking of alloantigen-specific CD8⁺ central memory T cells into lung allografts. We next set out to characterize further the behavior of CD8⁺ central memory T cells in immunosuppressed lung graft recipients. We observed that central memory CD8⁺ T lymphocytes that infiltrated grafts in costimulatory blockade–treated hosts have undergone proliferation, albeit to a lesser degree than in nonimmunosuppressed recipients (Supplemental Figure 4). To investigate their trafficking requirements, we generated donor-specific (anti-BALB/c) central memory CD45.1⁺CD8⁺ T cells in vitro and treated a portion of these cells with pertussis toxin (PTX), which irreversibly inactivates Gα$_i$-coupled chemokine receptor signaling. PTX-treated or untreated central memory CD8⁺ T cells were injected into immunosuppressed B6 recipients of BALB/c lungs and analyzed by flow cytometry 2 days later. We found that PTX treatment significantly impairs migration of donor-specific central memory CD8⁺ T lymphocytes into lung allograft tissue (Figure 9A). By contrast, PTX treatment did not alter trafficking of third-party–specific (anti-CBA/Ca) central memory CD8⁺ T cells into BALB/c allografts. Furthermore, compared with donor-specific cells, significantly fewer third-party–specific central memory CD8⁺ T lymphocytes infiltrated BALB/c lung allograft tissue (Figure 9A). This was not due to a global defect in cell migration, as similar numbers of anti-BALB/c and anti-CBA/Ca CD45.1⁺ B6 central memory CD8⁺ T cells infiltrated

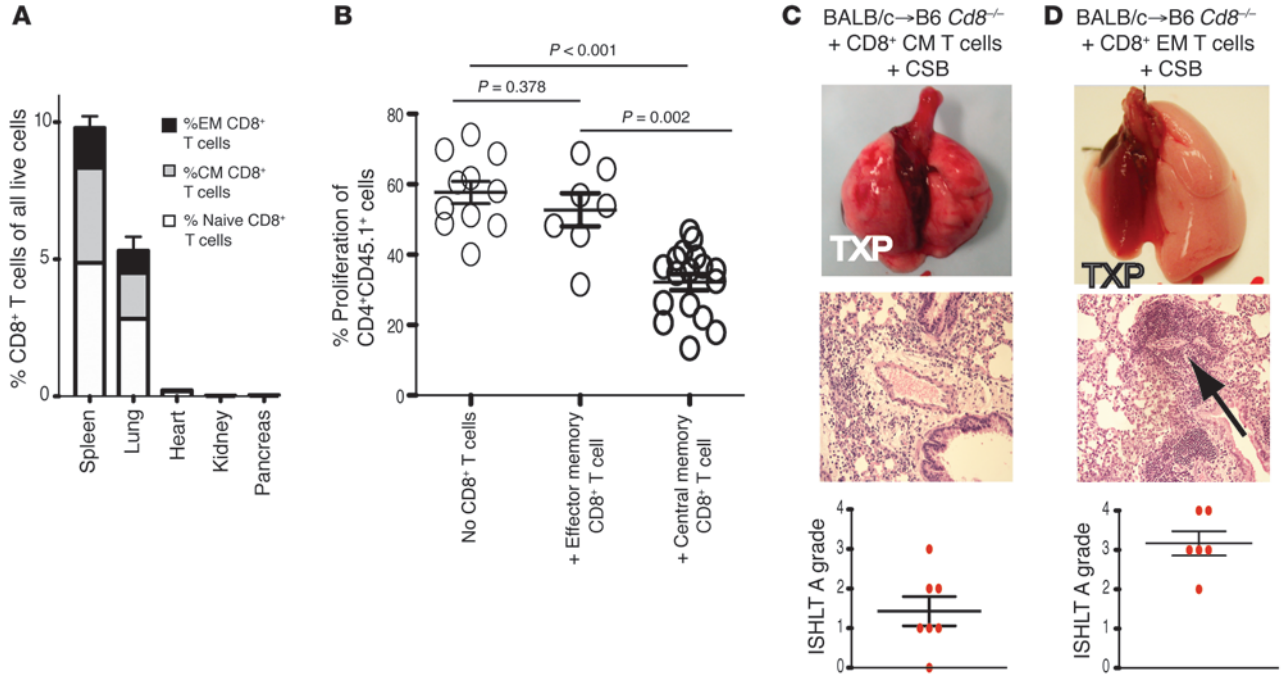

Figure 6

Central memory CD8+ T cells are abundant in the lung and can suppress alloimmune responses both in vitro and in vivo. (**A**) Compared with other solid organs, such as heart, kidney, and pancreas, the lung contains a relative abundance of CD8+ T lymphocytes, including central memory cells. Central memory (CM) cells are defined as $CD44^{hi}62L^{hi}$, effector memory (EM) cells are defined as $CD44^{hi}62L^{lo}$, and naive cells are defined as $CD44^{lo}62L^{hi}$. Data is representative of 4 separate animals. (**B**) Freshly isolated central memory CD8+ T cells from resting B6 mice suppress proliferation of B6 CD4+CD45.1+ T cells stimulated with BALB/c splenocytes using methodology similar to that described in Figure 4A. Pair-wise comparison between proliferation profiles of responder CD4+CD45.1+ T cells in wells containing no CD8+ T cells, effector memory CD8+ T cells, and central memory CD8+ T cells was performed by unpaired *t* test. (**C**) Adoptive transfer of in vitro–generated B6 anti-BALB/c central memory cells into B6 *Cd8*$^{-/-}$ recipients prevents rejection of BALB/c lung allografts after costimulatory blockade ($P = 0.751$ compared to Figure 2E by Mantel-Haenszel χ^2 test). (**D**) BALB/c lungs are rejected by B6 *Cd8*$^{-/-}$ recipient mice reconstituted with in vitro–generated anti-BALB/c CD8+ effector memory T lymphocytes despite costimulatory blockade ($P = 0.00105$ compared to Figure 2E by Mantel-Haenszel χ^2 test). TXP denotes graft, and the arrow points to perivascular infiltrates All gross and histological appearances as well as rejection grades represent grafts at 7 days after transplantation (original magnification, ×200 [histology, H&E staining]).

spleens of lung graft recipients (Supplemental Figure 5). Similar to central memory CD8+ T lymphocytes, graft infiltration of in vitro–generated anti-BALB/c CD8+ effector memory T cells was impaired after PTX treatment (Figure 9A). However, the absolute number of anti-donor effector memory T cells accumulating in the lung was significantly lower than that of anti-donor central memory T cells (Figure 9A). Collectively, these data suggest that chemokine receptor signaling as well as alloantigen recognition play a role in graft infiltration by CD8+ central memory T lymphocytes.

CCR7 expression on CD8+ T cells is critical for lung allograft acceptance. As the expression of the $G\alpha_i$-coupled chemokine receptor C-C chemokine receptor type 7+ (CCR7+) is a hallmark of central memory T cells, and a large portion of $CD8^+CD44^{hi}CD62L^{hi}$ T cells in accepting lung allografts express CCR7 (Figure 5A), we next explored whether this specific chemokine receptor plays a role in graft acceptance. We first transplanted BALB/c lungs into immunosuppressed CCR7-deficient recipients and observed that these grafts were acutely rejected (Supplemental Figure 6). As several cell populations in addition to T cells can express CCR7, we next focused on T lymphocytes by adoptively transferring B6 CCR7-deficient CD8+ T lymphocytes into costimulatory blockade–treated B6 *Cd8*$^{-/-}$ recipients of BALB/c lungs. Unlike immunosuppressed *Cd8*$^{-/-}$ recipients reconstituted with wild-type CD8+ T lymphocytes (Figure 2E), those reconstituted with *Ccr7*$^{-/-}$ CD8+ T cells acutely rejected BALB/c allografts (Figure 9B). This demonstrates that CCR7 expression on recipient CD8 T cells plays a critical role in mediating lung allograft acceptance. Having demonstrated that IFN-γ production by recipient CD8+ T cells is essential for lung allograft acceptance, we examined whether CCR7 expression on CD8 T cells regulates the production of this cytokine. Indeed, we found that local expression of *Ifng* was significantly decreased when graft-infiltrating CD8 T cells lacked CCR7 (Figure 9C).

We have shown previously that graft-infiltrating recipient CD11c+ cells in rejecting lung allografts express both donor and self–MHC class II molecules on their surface and can activate CD4+ T cells via both direct and indirect allorecognition (55). Similarly, graft-infiltrating recipient CD11c+ dendritic cells in accepting lungs express both donor and recipient MHC class I molecules (Figure 9D), suggesting that recipient dendritic cells can contribute to the activation of alloreactive CD8+ T cells through both direct and indirect pathways of alloantigen presentation (56). Furthermore, this cell population has been shown to express CCL21, a ligand for CCR7, on its surface (57). To further evaluate the role of CCR7 expression on CD8+ T cells, we took advantage of our recently

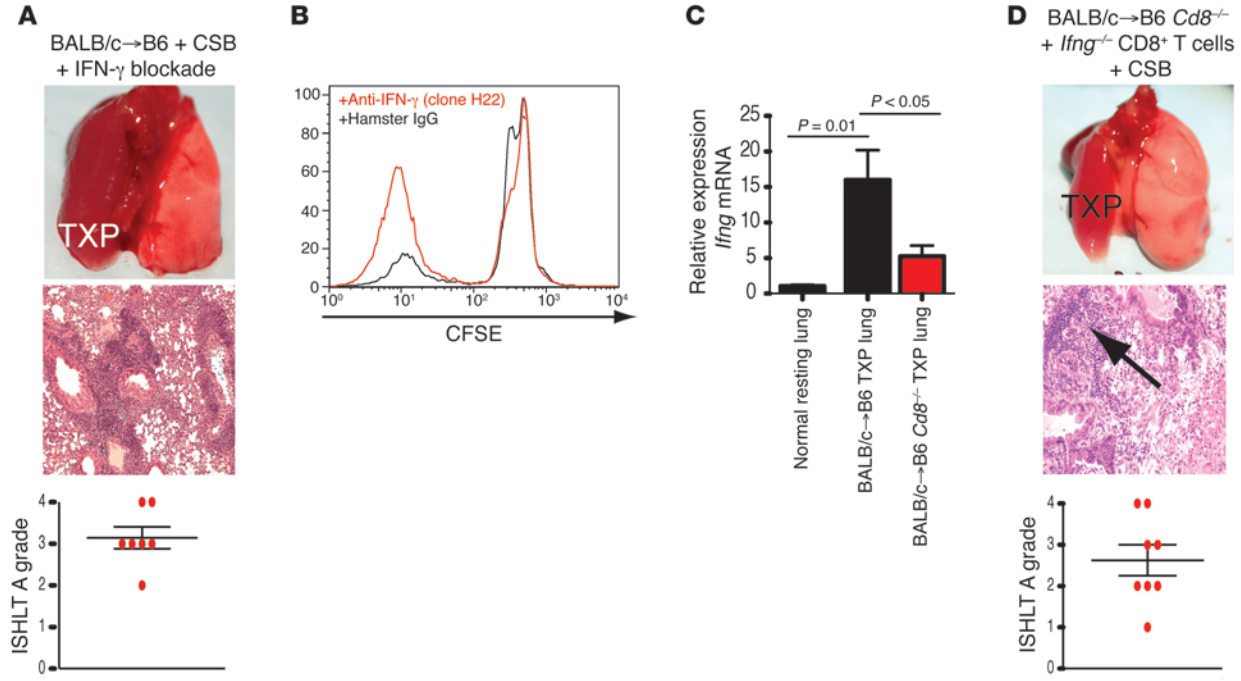

Figure 7

CD8⁺ T cell–mediated lung allograft acceptance is dependent on IFN-γ production. (**A**) Blocking IFN-γ prevents acceptance of BALB/c lung grafts by B6 recipients despite CSB. Gross appearance, histology, and ISHLT A rejection grade are shown (P = 0.000258 vs. Figure 2A by Mantel-Haenszel χ^2 test). (**B**) In vitro proliferation of CD4⁺CD45.1⁺ T cells (CFSE) stimulated by BALB/c splenocytes in the presence of accepting allograft-derived CD8⁺ T cells after addition of IFN-γ–blocking (red) or control antibody (black) (n = 3 separate experiments). (**C**) *Ifng* levels in allografts are significantly higher 4 days after transplantation into wild-type vs. *Cd8*$^{-/-}$ B6 recipients (n = 4 each; unpaired t test). (**D**) Injection of *Ifng*$^{-/-}$ CD8⁺ T cells does not restore lung allograft acceptance (P = 0.0066 vs. Figure 2E using Mantel-Haenszel χ^2 test). All gross and histological appearances as well as rejection grades represent grafts at 7 days after transplantation (original magnification, ×200 [histology, H&E staining]). TXP denotes graft, and the arrow points to perivascular infiltrates.

described method to image murine lungs by 2-photon microscopy in vivo (58). We transplanted BALB/c lungs into immunosuppressed B6 CD11c-EYFP hosts, which express enhanced yellow fluorescent protein under a CD11c promoter, and injected fluorescently labeled B6 CD8⁺ wild-type and *Ccr7*$^{-/-}$ T cells 3 days after engraftment. When we imaged these lung grafts 24 hours later, we observed that wild-type CD8⁺ T lymphocytes made stable and long-lasting contacts with graft-infiltrating recipient CD11c⁺ cells. By contrast, in the absence of CCR7 expression, CD8⁺ T cells interacted with CD11c⁺ dendritic cells only briefly, with significantly shorter retention times (P < 0.001) (Figure 10 and Supplemental Video 1). Collectively, these findings suggest that, in addition to directing trafficking of T lymphocytes into the lung, chemokine receptor signaling regulates contact between graft-infiltrating CD8⁺ T cells and alloantigen-expressing cells, which is associated with decreased local production of IFN-γ and graft rejection.

Discussion

The overwhelming success of costimulation blockade (CSB) in extending graft survival in small animal models of organ transplantation has laid the foundation for translating this therapy to the clinics (59). However, kidney transplantation experiments in nonhuman primates demonstrated that alloreactive memory T cells, generated through heterologous immunity, may represent a barrier to long-term graft survival in animals raised outside the confines of specific pathogen–free conditions (60, 61). This has been suspected to be especially problematic in recipients with a high frequency of CD8⁺ memory T cells, due to rapid graft infiltration by this cell population (13, 15). Based on these observations, strategies have been developed to either globally deplete T lymphocytes during the perioperative period (62) or specifically target memory T cells (21). We have previously reported that treatment of lung allograft recipients with CTLA4-Ig alone does not prevent acute rejection regardless of presence of CD4⁺ T cells (31). Additional treatment with anti-CD154 prevents rejection after transplantation of lungs into wild-type or even CD4⁺ T cell–depleted allogeneic hosts, possibly due to transient expression of this costimulatory molecule on CD8⁺ T lymphocytes or other cells (13, 63).

The unique features of the lung, such as the rapidity and local initiation of the immune response, have allowed us to unravel a previously unrecognized and critical role for CD8⁺CD44^{hi}CD62L^{hi} CCR7⁺ T cells in the induction of graft acceptance. We and others have shown that lungs provide a suitable environment for the activation of adaptive immunity in the absence of secondary lymphoid organs (64–66). Our recent studies have demonstrated that innate and adaptive immune cells rapidly infiltrate lung grafts and that their interactions within the graft determine the fate of this organ (58, 67). Of particular relevance to the current findings, we have shown recently that immune responses contributing to lung allograft acceptance are established locally in the graft shortly after transplantation (30), while other tissue and organ grafts require the presence of secondary lymphoid organs for the initia-

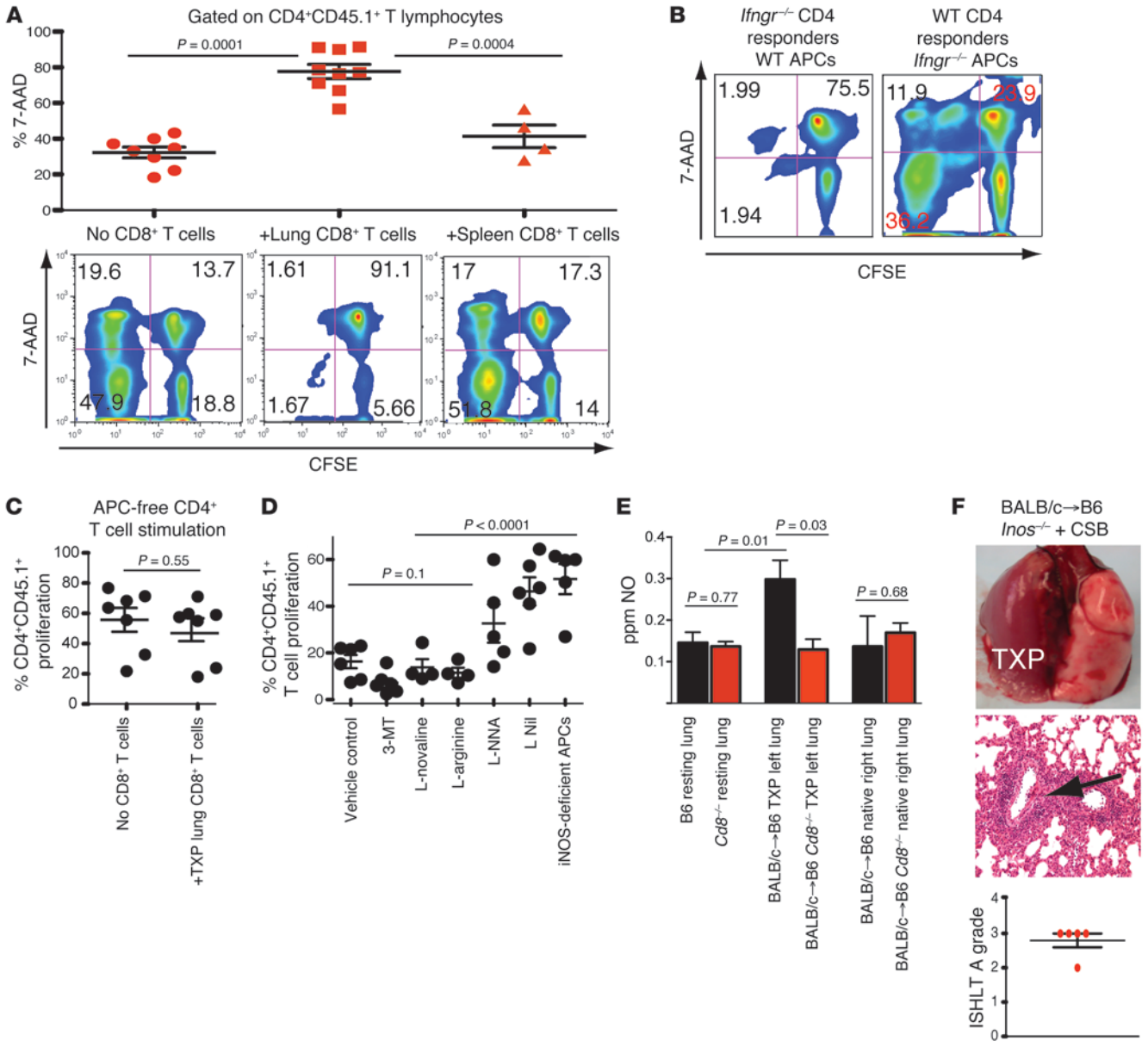

Figure 8

CD8+ T cells suppress through IFN-γ–mediated production of NO. (**A**) After 5 days, the majority of CD4+CD45.1+ T cell "responders" are not viable if CD8+ T cells from accepting allografts are added. CD4+CD45.1+ T cell viability (by 7-AAD uptake) and representative plots of CFSE vs. 7-AAD are shown (groups compared by unpaired *t* test). (**B**) CD4+ T cell proliferation (CFSE) and viability (7-AAD) in an MLR containing *Ifngr1*$^{-/-}$ CD4+ T cell responders or *Ifngr1*$^{-/-}$ antigen-presenting cells ($n \geq 3$). Numbers in density plots in **A** and **B** represent percentages of CD4+CD45.1+ T cells within the respective quadrants, assessing their proliferation (CFSE) vs. viability (7-AAD). (**C**) CD4+ T cell proliferation after stimulation with plate-bound anti-CD3 and soluble anti-CD28 in the absence or presence of accepting allograft-derived CD8+ T cells ($P = 0.55$ between the 2 groups by unpaired *t* test). (**D**) CD4+ T cell proliferation with inhibitors of amino acid metabolism, arginine, or *Inos*$^{-/-}$ antigen-presenting cells (multiple group comparison performed by ANOVA). (**E**) NO levels in resting lungs, allografts, and right native lungs ($n \geq 3$) (unpaired *t* test). (**F**) BALB/c lungs transplanted into CSB-treated *Inos*$^{-/-}$ B6 recipients ($P = 0.00059$ vs. Figure 2A by Mantel-Haenszel χ^2 test). TXP denotes graft, and the arrow points to perivascular infiltrates All gross and histological appearances as well as rejection grades represent grafts at 7 days after transplantation (original magnification, ×200 [histology, H&E staining]).

tion as well as downregulation of alloimmune responses (68–70). Our findings, with regard to trafficking requirements of CD8+ T cells to pulmonary allografts, further extend the notion that lungs differ immunologically from other transplanted organs. It has been demonstrated recently that antigen recognition regulates trafficking of effector CD8+ T cells into murine heart grafts (71). Consistent with these data, we now demonstrate that in vitro–generated central memory CD8+ T lymphocytes infiltrate lung allografts to a significantly larger extent compared with anti–third party central memory CD8+ T cells. However, in direct contrast to

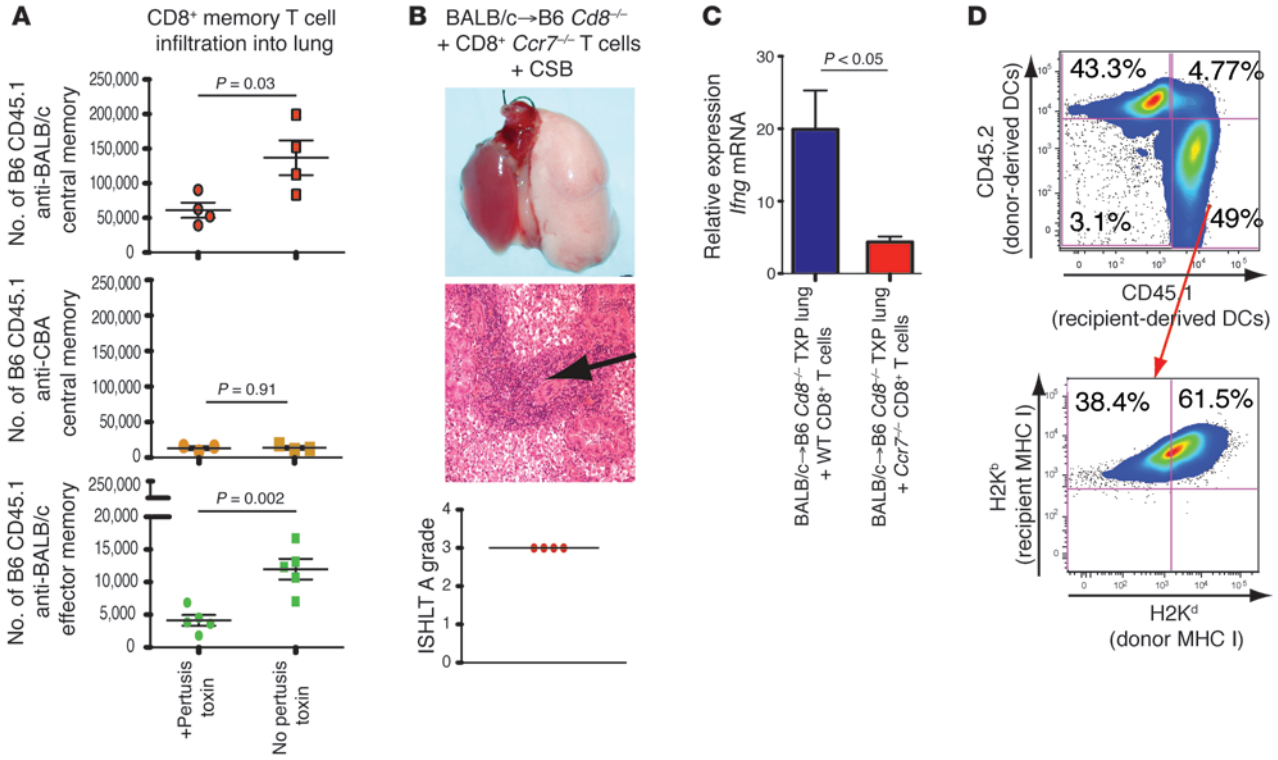

Figure 9

Chemokine receptor expression regulates CD8+ T cell–mediated lung acceptance. (**A**) Graft infiltration by PTX-treated or untreated anti-donor (BALB/c) central memory, anti–third party (CBA/Ca) central memory, or anti-donor (BALB/c) effector memory B6 CD8+CD45.1+ T cells (comparison within each group by unpaired *t* test). (**B**) Injection of *Ccr7*$^{-/-}$ CD8+ T cells does not restore allograft acceptance in B6 *Cd8*$^{-/-}$ recipients ($P = 0.00054$ vs. Figure 2E by Mantel-Haenszel χ^2 test). The arrow points to perivascular infiltrates. (**C**) Immunosuppressed BALB/c→B6 *Cd8*$^{-/-}$ recipients reconstituted with wild-type B6 CD8+ T cells ($n = 8$) had higher graft *Ifng* levels than those reconstituted with B6 *Ccr7*$^{-/-}$ CD8+ T cells ($n = 5$) (day 4) (unpaired *t* test). (**D**) Majority of recipient-derived graft-infiltrating CD11c+ cells in immunosuppressed BALB/c (CD45.2+)→B6 (CD45.1+) transplants express donor MHC class I (H-2K^d) ($n = 3$). Numbers in top density plot represent percentages of CD11c+ cells expressing CD45.1 (recipient) vs. CD45.2 (donor). Numbers in bottom density plot represent percentages of recipient CD45.1+CD45.2−CD11c+ cells expressing donor (H-2K^d) vs. recipient (H-2K^b) MHC class I. Representative of 3 independent experiments. All gross and histological appearances as well as rejection grades represent grafts at 7 days after transplantation (original magnification, ×200 [histology, H&E staining]).

heart allografts, we now demonstrate that Gα_1 receptor signaling is also critical for donor-primed CD8+ effector and central memory T cell infiltration into lung grafts. Our findings extend recent reports that chemokine receptor expression on T cells regulates their homing to virally infected lungs (72). We thus show that both alloantigen- and Gα_1-dependent chemokine signaling play a role in memory T lymphocyte migration into lungs.

Since their description almost 2 decades ago (73), the majority of studies investigating mechanisms of immune regulation have focused on CD4+Foxp3+ regulatory T cells (69). Despite experimental evidence dating back to the 1970s that CD8+ T cells can suppress immune responses, only recently has this cell population experienced a resurgence in the literature. This is in large part due to the phenotypic heterogeneity of CD8+ T cells with suppressive function. To this end, CD8+ T cells with both naive and memory phenotypes have been described to have regulatory capacity. Expansion of naive human CD8+CCR7+ T cells with low-dose anti-CD3 and IL-15 induces their expression of Foxp3, CD25, and CD103 and their ability to suppress activation of CD4+ T cells (74). In mice, CD8+ Foxp3+ T cells can regulate skin alloimmune responses in a contact-dependent fashion (43), and a similar population of cells that relies on direct interaction with CD4+ T cell responders has been described in humans (74). In rats, a regulatory CD8+Foxp3+CTLA4+ CD45RC^{lo} population has been described; however, controversy exists as to whether these cells suppress via production of cytokines or cell-to-cell contact (42, 75). Reports that CD8+ T cells can suppress through TGF-β also exist (48, 76). In contrast to these reports, we now describe an IFN-γ–dependent mechanism of CD8+CCR7+ T cell–mediated immunosuppression in the murine lung.

CCR7 expression is a hallmark of central memory T cells and regulates their homing to lymph nodes. Investigations into the role of CCR7 in transplant rejection have yielded conflicting results, which may be in part due to this molecule regulating migration and function of multiple cell populations. Hearts and skin experienced a moderate prolongation in survival after transplantation into *Ccr7*$^{-/-}$ recipients, which is associated with reduced T cell graft infiltration (77). Interrupting CCR7 signaling has been shown to enhance allograft survival through reduction of Th1 responses (78). Detrimental effects of recipient CCR7 deficiency on graft survival, on the other hand, have been attributed to decreased trafficking of tolerogenic antigen-presenting cells, such as plasmacytoid dendritic cells, into draining lymph nodes (79) or CD4+Foxp3+ T cells into grafts (80).

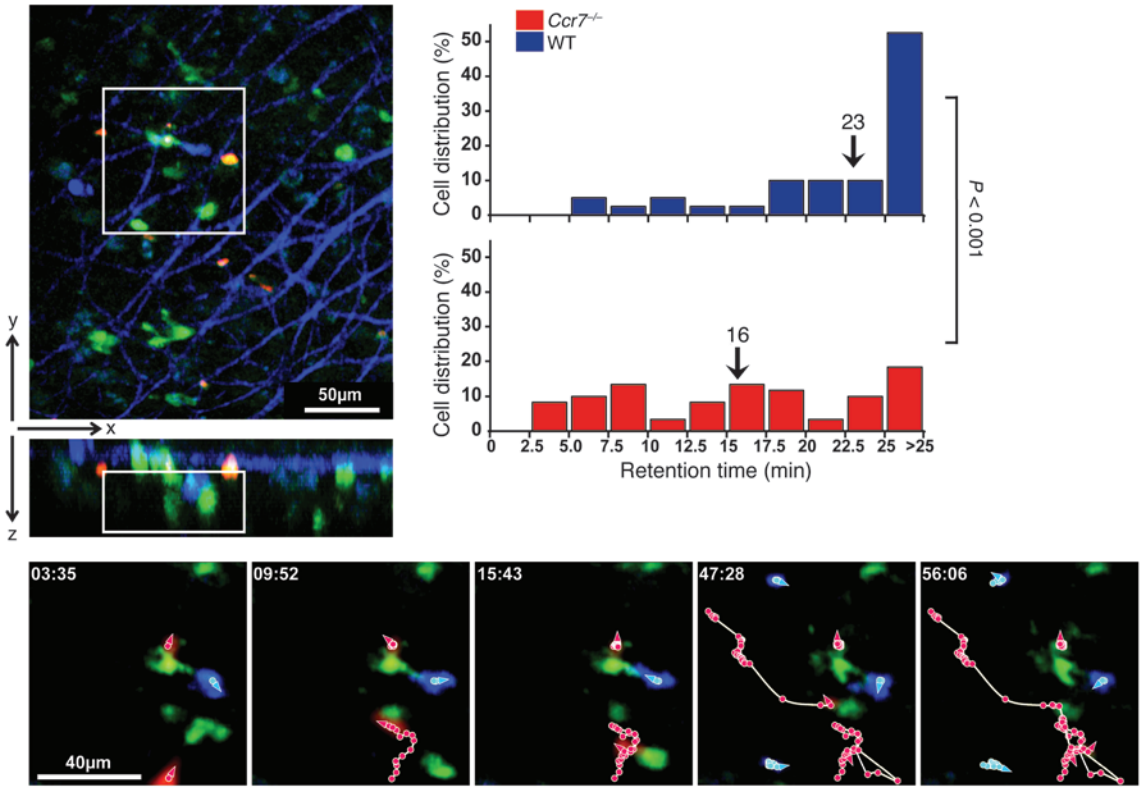

Figure 10
CCR7 expression on CD8⁺ T cells regulates their interactions with CD11c⁺ antigen-presenting cells within CSB-treated lung allografts. Intravital 2-photon microscopy demonstrating wild-type B6 CD8⁺ T cells (cyan), *Ccr7*$^{-/-}$ B6 CD8⁺ T cells (red), and CD11c⁺ cells (green) in immunosuppressed BALB/c→B6 CD11c-EYFP allografts on day 4. Collagen appears as blue. Higher-magnification views show representative T cell movement over a 1-hour interval. Cyan tracks follow the movement of wild-type CD8⁺ T cells, whereas red tracks follow *Ccr7*$^{-/-}$ CD8⁺ T cells. Scale bars: 50 μm (top); 40 μm (bottom). Images are individual frames from a continuous time-lapse recording (Supplemental Video 1). Relative time displayed in minutes/seconds. Boxed regions are shown at high magnification in bottom panels. Wild-type T cells (blue) have higher mean retention times (mostly associated with CD11c⁺ cells) than *Ccr7*$^{-/-}$ T cells (red) (23 vs. 16 minutes, $P < 0.001$, *t* test). Representative data are shown from two independent experiments with similar results.

Here, we report that CCR7-expressing CD8⁺ T cells are critical for lung allograft acceptance. Mechanistically, we show by intravital 2-photon microscopy that, in the absence of CCR7, CD8⁺ T cells are unable to form durable interactions with antigen-presenting cells within the graft, which is associated with lower expression of IFN-γ. These findings extend previous reports showing that dendritic cells express CCL21 and that surface-bound CCR7 ligands induce tethering of T lymphocytes to antigen-presenting cells during the formation of stable synapses (81, 82). It has also been shown that dendritic cells bind more CCR7 ligands on their surface than other cell populations (57). Previous reports have pointed to a role of CCR7 ligands in T cell differentiation. Stimulation of dendritic cells with CCR7 ligands induces their production of IL-12 and IL-23, which can drive Th1 and Th17 differentiation, respectively (83). Consistent with our findings, others have also observed that CCR7 expression on T cells is critical to mount an IFN-γ–dependent immune response that is required to clear pathogens (84).

Traditionally, Th1 responses have been considered to be instrumental in promoting cell-mediated rejection. We have described an accumulation of IFN-γ–producing CD4⁺ and CD8⁺ T cells in nonimmunosuppressed lung allografts that undergo acute rejection (31). Perhaps more importantly, excessive activation of Th1 responses due to ischemia/reperfusion injury abrogates immunosuppression-mediated lung graft acceptance (67). However, the absence of IFN-γ can also have deleterious effects on graft survival. Cardiac allografts undergo necrosis in the absence of recipient IFN-γ despite immunosuppression, which has been attributed to inefficient deletion of activated T lymphocytes (85). Activation of alternative pathways, such as the Th17 differentiation pathway, may also mediate aggressive proinflammatory responses in the absence of IFN-γ (86, 87).

As memory T lymphocytes in peripheral organs provide a first line of defense against infection, mucosal barrier organs, such as the lung, are especially rich in this cell population (88, 89). In fact, independent of antigen or inflammation, memory T cells are retained in lungs, in which they are rapid producers of proinflammatory cytokines (89, 90). As uncontrolled inflammatory responses in the lung can result in potentially life-threatening pulmonary dysfunction, mechanisms have evolved that limit the extent of inflammation to prevent tissue damage (91). For example, iNOS limits pulmonary inflammation in several models of lung injury (92, 93). Thus, it is possible that our costimulatory blockade protocol relies on a naturally occurring IFN-γ– and NO-dependent "feedback mechanism" normally operational in the lung. In contrast to central memory CD8⁺ T cells, effector memory CD8⁺ T cells do not promote

lung allograft acceptance and are associated with graft rejection. Our findings support the notion that these 2 cell populations are functionally distinct (45). CCR7$^-$ effector memory T cells rapidly infiltrate peripheral tissues during inflammation and are rich in effector molecules, such as granzyme B, and surface killer cell lectin-like receptor family members, such as KLRG1 (94, 95). CCR7$^+$ central memory T cells, however, have been traditionally described to reside in secondary lymphoid tissue and mediate delayed effector function through secretion of proinflammatory cytokines such as IFN-γ (50). Thus, it is possible that the unique physiology of the lung, which is enriched in central memory cells compared with other organs, relies on cytokine production by this cell population to downregulate immune responses. Since central memory CD8$^+$ T cells that infiltrate accepting lung allografts have undergone proliferation, we speculate that expansion of this cell population is needed to prevent rejection.

Our findings provide an impetus to critically evaluate current immunosuppressive strategies used in clinical lung transplantation, as many of them actually inhibit the pathways that we have identified as necessary for lung transplant acceptance. Examples include global T cell depletion, which would eliminate central memory CD8 T cells; mycophenolic acid, which inhibits early Th1 responses (96); and calcineurin inhibitors, which have been shown to suppress iNOS (97). New approaches, such as ex vivo lung perfusion, have the potential to test these findings in preclinical models (98).

Methods

Animals. Wild-type, *Ifng*$^{-/-}$, *Ifngr1*$^{-/-}$, *Ccr7*$^{-/-}$, *Cd8*$^{-/-}$, *Inos*$^{-/-}$, *Tnfa*$^{-/-}$, CD11c-EYFP, CD45.1$^+$, and B cell–deficient (*Ighm*$^{-/-}$) mice, all on a B6 (H-2K^b) background, as well as BALB/c (H-2K^d), CBA/Ca (H2K^k), and nude mice were purchased from The Jackson Laboratory. Animals were housed in a barrier facility in air-filtered cages. Left orthotopic vascularized lung transplants were performed as previously described (40) with CSB in select experiments consisting of MR1 (250 μg i.p., day 0) and CTLA4-Ig (200 μg i.p., day 2). As indicated for select experiments, CD8$^+$ T cells were depleted in vivo by YTS 169.1 (250 μg i.p., days –3, –1), IFN-γ was neutralized using hamster anti-mouse anti–IFN-γ antibody (clone H22) (500 g day –2, 250 μg i.p. day –1), and CD4$^+$ T cells were depleted using GK1.5 (100 μg i.p., days –3, –1). For select experiments, OX40/OX40 ligand (clone OX-86), CD27/CD70 (clone FR-70), and ICOS/ICOS ligand (clone 17G9) pathways were inhibited as previously described (all antibodies from BioXcell) (41). For some experiments, nude mice were reconstituted with 10^7 CD4$^+$ T cells isolated from the spleens and peripheral lymph nodes of B6 wild-type mice and, for others, CFSE-labeled CD4$^+$CD45.1$^+$ T cells were adoptively transferred into B6 mice. Reconstitution of B6 *Cd8*$^{-/-}$ mice was performed with a minimum of 5×10^6 CD8$^+$ T cells isolated either by flow cytometric sorting or magnetic bead isolation (Miltenyi Biotech).

Memory cell generation and injection. Both central and effector memory CD8$^+$ T cells were generated in vitro based on previously described methods (50, 51). Briefly, central memory cells were generated by coculturing B6 CD45.1$^+$ splenocytes with irradiated BALB/c (donor) or CBA/Ca (third party) splenocyte stimulators. Sixty hours after initiation of the cocultures dead cells were removed by Ficoll-Paque density centrifugation and CD8$^+$ T cells were positively selected with magnetic beads. CD8$^+$ T cells were then expanded in 20 ng/ml IL-15 (R&D Systems) and injected intravenously approximately 2 weeks later. Effector memory cells were generated by coculturing B6 CD45.1$^+$ splenocytes with irradiated BALB/c stimulators in the presence of 1,000 U/ml IL-2 (NIH NCI-Clinical Repository). For homing studies, 5×10^6 effector memory cells and 1×10^6 central memory cells were injected per mouse 2 to 3 days after transplantation. For reconstitution experiments, B6 *Cd8*$^{-/-}$ mice were injected with 5×10^6 effector or central memory cells 48 to 72 hours prior to BALB/c lung allograft transplantation. For some experiments, memory cells were treated with 200 ng/ml PTX for 30 minutes prior to injection. For homing studies, lung grafts were flushed with 2.5 ml sterile saline prior to analysis

Histology. Transplanted mouse lungs were fixed in formaldehyde, sectioned, and stained with H&E. A lung pathologist (J.H. Ritter) blinded to the experimental conditions graded graft rejection using standard criteria (International Society for Heart and Lung Transplantation [ISHLT] A Grade) developed by the Lung Rejection Study Group (32).

Flow cytometry. All antibodies for flow cytometry were primarily fluorochrome conjugated and purchased from eBioscience. Intracellular staining was performed as previously described (31).

In vitro MLRs. In vitro MLRs were performed in round bottom 96-well plates using 3×10^5 T cell–depleted BALB/c splenocyte stimulators, with 10^5 CFSE-labeled B6 CD45.1$^+$CD4$^+$ or CD8$^+$ T cell responders and, as indicated above, 10^5 CD8$^+$ T cells isolated from lungs or spleens of immunosuppressed B6 recipients of BALB/c allografts. For some experiments, central and effector memory T cells were sorted from lungs of resting mice. T cell responses were evaluated flow cytometrically on day 5. All compounds inhibiting the metabolism of essential amino acids were obtained from Sigma-Aldrich and added to the cocultures as previously described for the duration of the experiment (41).

Quantitative gene expression analysis. For quantitative gene expression analysis, mRNA from whole lung grafts was isolated in accordance with the manufacturer's instructions. Quantitative real-time RT-PCR was conducted on an ABI 7900 using TaqMan Gene Expression Assay system (Applied Biosystems) in accordance with the manufacturer's recommendations. Amplification of target sequences was conducted as follows: 50°C for 20 minutes and 95°C for 10 minutes, followed by 38 to 45 cycles of 95°C for 15 seconds and 60°C for 1 minute. Primers and MGB probes were purchased as kits from Applied Biosystems and can be identified in the following manner: IFN-γ (Mm01168134_m1) and β-2 microglobulin (Mm00437762_m1). Transcript levels of IFN-γ are expressed relative to transcript levels of β-2 microglobulin.

NO measurement in vivo. In vivo experiments were carried out using a 2 mm NO Sensor (World Precision Instruments) connected to a Free Radical Analyzer TBR-1025 (World Precision Instruments). The specifications include a 2 pA/nM sensitivity with a 1 nM minimum detection limit. Prior to the experiments, the sensor was polarized for at least 24 hours before use according to the manufacturer's recommendations. After sedating the mouse, a 2 mm long and 1 mm deep incision was made in the lung tissue to provide an area for the sensor to rest in. Approximately 0.5 ml saline was applied to the incision in order to provide an interface between the mouse lung and sensor and also to monitor the integrity of the sensor's NO-selective membrane. The data from each lung were recorded using a LabTrax data acquisition unit and LabScribe software for 5 minutes after reaching a stable signal. The data were then analyzed against a baseline signal from normal saline and converted from current to NO concentration in ppm using NO donor DEA-Nonoate (Cayman Chemical) dissolved in PBS buffer as a standard.

Immunostaining. Lungs were cryopreserved and then cut into 6-μm-thick sections. Sections were fixed in pure acetone for 10 minutes at –20°C and blocked with 10% normal donkey serum. Unlabeled anti-CD4 (H129.19) and anti-CD8 (53-6.7) (Pharmingen) were visualized using donkey anti-rat IgG conjugated with indocarbocyanine (Cy3) (Roche). Slides were imaged using an Olympus BX51 microscope. No detectable staining was observed with isotype-matched or species-specific control antibodies.

Intravital 2-photon microscopy. BALB/c lungs were transplanted into immunosuppressed B6 CD11c-EYFP recipients and, on postoperative day 3, received an injection of 10^7 CMTMR-labeled *Ccr7*$^{-/-}$ and 10^7 CD8$^+$ T cells isolated from wild-type B6 mice expressing cyan fluorescent protein under an actin promoter. Twenty-four hours after injection of T cells, time-lapse

imaging was performed with a custom-built 2-photon microscope running ImageWarp version 2.1 acquisition software (A&B Software). For time-lapse imaging of T cell–CD11c$^+$ dendritic cell interactions in lung tissue, we averaged 15 video-rate frames (0.5 seconds per slice) during the acquisition to match the ventilator rate and to minimize movement artifacts. Each plane represents an image of 220 × 240 μm in the x and y dimensions. Twenty-one sequential planes were acquired in the z dimension (2.5 μm each) to form a z stack. Each individual T cell was tracked from its first appearance in the imaging window and followed up to the time point at which it dislocated more than 20 μm from its starting position. T cells that did not travel were tracked for the duration of the imaging period.

Statistics. Continuous variables, such as in vitro and in vivo T cell proliferation, gene expression levels, retention times of T cells, number of memory T cells penetrating lung grafts, and NO levels, were compared among various conditions. Two-tailed Student's *t* test was used for 2 comparisons and ANOVA was used for multiple comparisons, as indicated in the appropriate figure legends. For ordinal variables, such as lung allograft rejection scores, the Mantel-Haenszel χ^2 test was used. Data in figures are presented as mean ± SEM. A *P* value of more than 0.05 is assumed to be not statistically significant.

Study approval. All animal procedures were approved by the Animal Studies Committee at Washington University School of Medicine, St. Louis, Missouri, USA.

Acknowledgments

This work was supported by the American Association for Thoracic Surgery, NIH (K08CA131097, R01HL113931, K08HL083983, R01HL094601, R01HL113436, HHSN268201000046C); the Thoracic Surgery Foundation for Research and Education; the American Thoracic Society Lungevity Foundation Research Grant; the American Cancer Society; the Foundation for Barnes Jewish Hospital; and the ISHLT. Experimental support was provided by the Facility of the Rheumatic Diseases Core Center under award number P30AR048335, the Siteman Cancer Center Flow Cytometry Core Facility under NCI Cancer Center Support Grant P30 CA91842, and the Biostatistics Core of the Siteman Cancer Center.

Received for publication June 5, 2013, and accepted in revised form December 5, 2013.

Address correspondence to: Alexander S. Krupnick or Daniel Kreisel, Campus Box 8234, 660 South Euclid Avenue, Washington University in St. Louis, St. Louis, Missouri 63110-1013, USA. Phone: 314.362.9181; Fax: 314.367.8459; krupnicka@wudosis.wustl.edu (A.S. Krupnick). Phone: 314.362.6023; Fax: 314.367.8459; E-mail: kreiseld@wudosis.wustl.edu (D. Kreisel).

1. Serraino D, et al. Risk of cancer following immunosuppression in organ transplant recipients and in HIV-positive individuals in southern Europe. *Eur J Cancer*. 2007;43(14):2117–2123.
2. Cervera C, Linares L, Bou G, Moreno A. Multidrug-resistant bacterial infection in solid organ transplant recipients. *Enferm Infecc Microbiol Clin*. 2012; 30(suppl 2):40–48.
3. Larsen CP, et al. Long-term acceptance of skin and cardiac allografts after blocking CD40 and CD28 pathways. *Nature*. 1996;381(6581):434–438.
4. Banuelos SJ, et al. Regulation of skin and islet allograft survival in mice treated with costimulation blockade is mediated by different CD4+ cell subsets and different mechanisms. *Transplantation*. 2004;78(5):660–667.
5. Markees TG, et al. Long-term survival of skin allografts induced by donor splenocytes and anti-CD154 antibody in thymectomized mice requires CD4(+) T cells, interferon-γ, and CTLA4. *J Clin Invest*. 1998; 101(11):2446–2455.
6. Mease P, et al. Abatacept in the treatment of patients with psoriatic arthritis: results of a six-month, multicenter, randomized, double-blind, placebo-controlled, phase II trial. *Arthritis Rheum*. 2011;63(4):939–948.
7. Schiff M. Abatacept treatment for rheumatoid arthritis. *Rheumatology (Oxford)*. 2011;50(3):437–449.
8. Vincenti F, et al. A phase III study of belatacept-based immunosuppression regimens versus cyclosporine in renal transplant recipients (BENEFIT study). *Am J Transplant*. 2011;10(3):535–546.
9. Kreisel D, et al. Short- and long-term outcomes of 1000 adult lung transplant recipients at a single center. *J Thorac Cardiovasc Surg*. 2011;141(1):215–222.
10. Shah PD, McDyer JF. Viral infections in lung transplant recipients. *Semin Respir Crit Care Med*. 2010; 31(2):243–254.
11. Husain S, et al. Experience with immune monitoring in lung transplant recipients: correlation of low immune function with infection. *Transplantation*. 2009;87(12):1852–1857.
12. Adams AB, et al. Heterologous immunity provides a potent barrier to transplantation tolerance. *J Clin Invest*. 2003;111(12):1887–1895.
13. Zhai Y, Meng L, Gao F, Busuttil RW, Kupiec-Weglinski JW. Allograft rejection by primed/memory CD8+ T cells is CD154 blockade resistant: therapeutic implications for sensitized transplant recipients. *J Immunol*. 2002;169(8):4667–4673.
14. Trambley J, et al. Asialo GM1(+) CD8(+) T cells play a critical role in costimulation blockade-resistant allograft rejection. *J Clin Invest*. 1999;104(12):1715–1722.
15. Schenk AD, Nozaki T, Rabant M, Valujskikh A, Fairchild RL. Donor-reactive CD8 memory T cells infiltrate cardiac allografts within 24-h posttransplant in naive recipients. *Am J Transplant*. 2008; 8(8):1652–1661.
16. Schenk AD, Gorbacheva V, Rabant M, Fairchild RL, Valujskikh A. Effector functions of donor-reactive CD8 memory T cells are dependent on ICOS induced during division in cardiac grafts. *Am J Transplant*. 2009;9(1):64–73.
17. Koyama I, et al. Depletion of CD8 memory T cells for induction of tolerance of a previously transplanted kidney allograft. *Am J Transplant*. 2007; 7(5):1055–1061.
18. Donckier V, et al. Expansion of memory-type CD8+ T cells correlates with the failure of early immunosuppression withdrawal after cadaver liver transplantation using high-dose ATG induction and rapamycin. *Transplantation*. 2013;96(3):306–315.
19. Ascon M, et al. Renal ischemia-reperfusion leads to long term infiltration of activated and effector-memory T lymphocytes. *Kidney Int*. 2009;75(5):526–535.
20. Lo DJ, et al. Selective targeting of human alloresponsive CD8+ effector memory T cells based on CD2 expression. *Am J Transplant*. 2011;11(1):22–33.
21. Weaver TA, et al. Alefacept promotes co-stimulation blockade based allograft survival in nonhuman primates. *Nat Med*. 2009;15(7):746–749.
22. Dai H, Wan N, Zhang S, Moore Y, Wan F, Dai Z. Cutting edge: programmed death-1 defines CD8+CD122+ T cells as regulatory versus memory T cells. *J Immunol*. 2010;185(2):803–807.
23. Bahri R, Bollinger A, Bollinger T, Orinska Z, Bulfone-Paus S. Ectonucleotidase CD38 demarcates regulatory, memory-like CD8+ T cells with IFN-gamma-mediated suppressor activities. *PLoS One*. 2012;7(9):e45234.
24. Dubois A, et al. Regulation of Th2 responses and allergic inflammation through bystander activation of CD8+ T lymphocytes in early life. *J Immunol*. 2010;185(2):884–891.
25. Berry GJ, et al. The ISHLT working formulation for pathologic diagnosis of antibody-mediated rejection in heart transplantation: evolution and current status (2005–2011). *J Heart Lung Transplant*. 2011;30(6):601–611.
26. Maier S, et al. Inhibition of natural killer cells results in acceptance of cardiac allografts in CD28$^{-/-}$ mice. *Nat Med*. 2001;7(5):557–562.
27. McNerney ME, et al. Role of natural killer cell subsets in cardiac allograft rejection. *Am J Transplant*. 2006;6(3):505–513.
28. Nozaki T, et al. Antibody-mediated rejection of cardiac allografts in CCR5-deficient recipients. *J Immunol*. 2007;179(8):5238–5245.
29. Okazaki M, et al. Maintenance of airway epithelium in acutely rejected orthotopic vascularized mouse lung transplants. *Am J Respir Cell Mol Biol*. 2007;37(6):625–630.
30. Li W, et al. Lung transplant acceptance is facilitated by early events in the graft and is associated with lymphoid neogenesis. *Mucosal Immunol*. 2012; 5(5):544–554.
31. Gelman AE, et al. CD4+ T lymphocytes are not necessary for the acute rejection of vascularized mouse lung transplants. *J Immunol*. 2008;180(7):4754–4762.
32. Yousem SA, et al. Revision of the 1990 working formulation for the classification of pulmonary allograft rejection: Lung Rejection Study Group. *J Heart Lung Transplant*. 1996;15(1 pt 1):1–15.
33. Yamamoto S, et al. Cutting edge: Pseudomonas aeruginosa abolishes established lung transplant tolerance by stimulating B7 expression on neutrophils. *J Immunol*. 2012;189(9):4221–4225.
34. Rigby MR, Trexler AM, Pearson TC, Larsen CP. CD28/CD154 blockade prevents autoimmune diabetes by inducing nondeletional tolerance after effector t-cell inhibition and regulatory T-cell expansion. *Diabetes*. 2008;57(10):2672–2683.
35. Waldmann H, Cobbold S. Regulating the immune response to transplants. a role for CD4+ regulatory cells? *Immunity*. 2001;14(4):399–406.
36. Lee I, Wang L, Wells AD, Dorf ME, Ozkaynak E, Hancock WW. Recruitment of Foxp3+ T regulatory cells mediating allograft tolerance depends on the CCR4 chemokine receptor. *J Exp Med*. 2005; 201(7):1037–1044.
37. Iwakoshi NN, Mordes JP, Markees TG, Phillips NE, Rossini AA, Greiner DL. Treatment of allograft recipients with donor-specific transfusion and anti-CD154 antibody leads to deletion of alloreactive CD8+ T cells and prolonged graft survival in a CTLA4-dependent manner. *J Immunol*. 2000;164(1):512–521.

38. Walsh PT, Taylor DK, Turka LA. Tregs and transplantation tolerance. *J Clin Invest*. 2004;114(10):1398–1403.
39. Redfield RR, et al. Essential role for B cells in transplantation tolerance. *Curr Opin Immunol*. 2011; 23(5):685–691.
40. Okazaki M, et al. A mouse model of orthotopic vascularized aerated lung transplantation. *Am J Transplant*. 2007;7(6):1672–1679.
41. Habicht A, Najafian N, Yagita H, Sayegh MH, Clarkson MR. New insights in CD28-independent allograft rejection. *Am J Transplant*. 2007;7(8):1917–1926.
42. Xystrakis E, et al. Identification of a novel natural regulatory CD8 T-cell subset and analysis of its mechanism of regulation. *Blood*. 2004;104(10):3294–3301.
43. Lerret NM, Houlihan JL, Kheradmand T, Pothoven KL, Zhang ZJ, Luo X. Donor-specific CD8+ Foxp3+ T cells protect skin allografts and facilitate induction of conventional CD4+ Foxp3+ regulatory T cells. *Am J Transplant*. 2012;12(9):2335–2347.
44. Correale J, Villa A. Role of CD8+ CD25+ Foxp3+ regulatory T cells in multiple sclerosis. *Ann Neurol*. 2010;67(5):625–638.
45. Sallusto F, Lenig D, Forster R, Lipp M, Lanzavecchia A. Two subsets of memory T lymphocytes with distinct homing potentials and effector functions. *Nature*. 1999;401(6754):708–712.
46. Ford ML, Kirk AD, Larsen CP. Donor-reactive T-cell stimulation history and precursor frequency: barriers to tolerance induction. *Transplantation*. 2009;87(9 suppl):S69–S74.
47. Bingaman AW, Farber DL. Memory T cells in transplantation: generation, function, and potential role in rejection. *Am J Transplant*. 2004;4(6):846–852.
48. Wan N, Dai H, Wang T, Moore Y, Zheng XX, Dai Z. Bystander central memory but not effector memory CD8+ T cells suppress allograft rejection. *J Immunol*. 2008;180(1):113–121.
49. Ely KH, Cookenham T, Roberts AD, Woodland DL. Memory T cell populations in the lung airways are maintained by continual recruitment. *J Immunol*. 2006;176(1):537–543.
50. Weninger W, Crowley MA, Manjunath N, von Andrian UH. Migratory properties of naive, effector, and memory CD8(+) T cells. *J Exp Med*. 2001; 194(7):953–966.
51. Ophir E, et al. Murine anti-third-party central-memory CD8(+) T cells promote hematopoietic chimerism under mild conditioning: lymph-node sequestration and deletion of anti-donor T cells. *Blood*. 2012;121(7):1220–1228.
52. Cobbold SP, et al. Infectious tolerance via the consumption of essential amino acids and mTOR signaling. *Proc Natl Acad Sci U S A*. 2009; 106(29):12055–12060.
53. Geller DA, et al. Cytokines, endotoxin, and glucocorticoids regulate the expression of inducible nitric oxide synthase in hepatocytes. *Proc Natl Acad Sci U S A*. 1993;90(2):522–526.
54. Purushothaman D, Marcel N, Garg M, Venkataraman R, Sarin A. Apoptotic programs are determined during lineage commitment of CD4+ T effectors: selective regulation of T effector-memory apoptosis by inducible nitric oxide synthase. *J Immunol*. 2013;190(1):97–105.
55. Gelman AE, et al. CCR2 regulates monocyte recruitment as well as CD4 T1 allorecognition after lung transplantation. *Am J Transplant*. 2010; 10(5):1189–1199.
56. Rogers NJ, Lechler RI. Allorecognition. *Am J Transplant*. 2001;1(2):97–102.
57. Friedman RS, Jacobelli J, Krummel MF. Surface-bound chemokines capture and prime T cells for synapse formation. *Nat Immunol*. 2006;7(10):1101–1108.
58. Kreisel D, et al. In vivo two-photon imaging reveals monocyte-dependent neutrophil extravasation during pulmonary inflammation. *Proc Natl Acad Sci U S A*. 2010;107(42):18073–18078.
59. Vincenti F, et al. Three-year outcomes from BENEFIT, a randomized, active-controlled, parallel-group study in adult kidney transplant recipients. *Am J Transplant*. 2012;12(1):210–217.
60. Lo DJ, et al. Belatacept and sirolimus prolong nonhuman primate renal allograft survival without a requirement for memory T cell depletion. *Am J Transplant*. 2013;13(2):320–328.
61. Nadazdin O, et al. Host alloreactive memory T cells influence tolerance to kidney allografts in nonhuman primates. *Sci Transl Med*. 2011;3(86):86ra51.
62. Padiyar A, Augustine JJ, Hricik DE. Induction antibody therapy in kidney transplantation. *Am J Kidney Dis*. 2009;54(5):935–944.
63. Mackey MF, Barth RJ, Barth RJ Jr, Noelle RJ. The role of CD40/CD154 interactions in the priming, differentiation, and effector function of helper and cytotoxic T cells. *J Leukoc Biol*. 1998;63(4):418–428.
64. Moyron-Quiroz JE, et al. Persistence and responsiveness of immunologic memory in the absence of secondary lymphoid organs. *Immunity*. 2006; 25(4):643–654.
65. Moyron-Quiroz JE, et al. Role of inducible bronchus associated lymphoid tissue (iBALT) in respiratory immunity. *Nat Med*. 2004;10(9):927–934.
66. Gelman AE, et al. Cutting edge: Acute lung allograft rejection is independent of secondary lymphoid organs. *J Immunol*. 2009;182(7):3969–3973.
67. Kreisel D, et al. Emergency granulopoiesis promotes neutrophil-dendritic cell encounters that prevent mouse lung allograft acceptance. *Blood*. 2011;118(23):6172–6182.
68. Barker CF, Billingham RE. The role of afferent lymphatics in the rejection of skin homografts. *J Exp Med*. 1968;128(1):197–221.
69. Zhang N, et al. Regulatory T cells sequentially migrate from inflamed tissues to draining lymph nodes to suppress the alloimmune response. *Immunity*. 2009;30(3):458–469.
70. Lakkis FG, Arakelov A, Konieczny BT, Inoue Y. Immunologic 'ignorance' of vascularized organ transplants in the absence of secondary lymphoid tissue. *Nat Med*. 2000;6(6):686–688.
71. Walch JM, et al. Cognate antigen directs CD8+ T cell migration to vascularized transplants. *J Clin Invest*. 2013;123(6):2663–2671.
72. Mikhak Z, Strassner JP, Luster AD. Lung dendritic cells imprint T cell lung homing and promote lung immunity through the chemokine receptor CCR4. *J Exp Med*. 2013;210(9):1855–1869.
73. Sakaguchi S, Sakaguchi N, Asano M, Itoh M, Toda M. Immunologic self-tolerance maintained by activated T cells expressing IL-2 receptor alpha-chains (CD25). Breakdown of a single mechanism of self-tolerance causes various autoimmune diseases. *J Immunol*. 1995;155(3):1151–1164.
74. Suzuki M, et al. CD8+CD45RA+CCR7+FOXP3+ T cells with immunosuppressive properties: a novel subset of inducible human regulatory T cells. *J Immunol*. 2012;189(5):2118–2130.
75. Guillonneau C, et al. CD40Ig treatment results in allograft acceptance mediated by CD8CD45RC T cells, IFN-γ, and indoleamine 2,3-dioxygenase. *J Clin Invest*. 2007;117(4):1096–1106.
76. Myers L, Croft M, Kwon BS, Mittler RS, Vella AT. Peptide-specific CD8 T regulatory cells use IFN-γ to elaborate TGF-β-based suppression. *J Immunol*. 2005;174(12):7625–7632.
77. Beckmann JH, et al. Prolongation of allograft survival in ccr7-deficient mice. *Transplantation*. 2004;77(12):1809–1814.
78. Ziegler E, et al. CCL19-IgG prevents allograft rejection by impairment of immune cell trafficking. *J Am Soc Nephrol*. 2006;17(9):2521–2532.
79. Liu X, et al. Tolerance induction towards cardiac allografts under costimulation blockade is impaired in CCR7-deficient animals but can be restored by adoptive transfer of syngeneic plasmacytoid dendritic cells. *Eur J Immunol*. 2011;41(3):611–623.
80. Gregson AL, et al. Protection against bronchiolitis obliterans syndrome is associated with allograft CCR7+ CD45RA– T regulatory cells. *PLoS One*. 2010; 5(6):e11354.
81. Kaiser A, Donnadieu E, Abastado JP, Trautmann A, Nardin A. CC chemokine ligand 19 secreted by mature dendritic cells increases naive T cell scanning behavior and their response to rare cognate antigen. *J Immunol*. 2005;175(4):2349–2356.
82. Ngo VN, Tang HL, Cyster JG. Epstein-Barr virus-induced molecule 1 ligand chemokine is expressed by dendritic cells in lymphoid tissues and strongly attracts naive T cells and activated B cells. *J Exp Med*. 1998;188(1):181–191.
83. Kuwabara T, et al. CCR7 ligands are required for development of experimental autoimmune encephalomyelitis through generating IL-23-dependent Th17 cells. *J Immunol*. 2009;183(4):2513–2521.
84. Noor S, et al. CCR7-dependent immunity during acute Toxoplasma gondii infection. *Infect Immun*. 2010;78(5):2257–2263.
85. Konieczny BT, et al. IFN-γ is critical for long-term allograft survival induced by blocking the CD28 and CD40 ligand T cell costimulation pathways. *J Immunol*. 1998;160(5):2059–2064.
86. Yuan X, et al. A novel role of CD4 Th17 cells in mediating cardiac allograft rejection and vasculopathy. *J Exp Med*. 2008;205(13):3133–3144.
87. Sis B, Famulski KS, Allanach KL, Zhu LF, Halloran PF. IFN-gamma prevents early perforin-granzyme-mediated destruction of kidney allografts by inducing donor class I products in the kidney. *Am J Transplant*. 2007;7(10):2301–2310.
88. Sheridan BS, Lefrancois L. Regional and mucosal memory T cells. *Nat Immunol*. 2011;12(6):485–491.
89. Sathaliyawala T, et al. Distribution and compartmentalization of human circulating and tissue-resident memory T cell subsets. *Immunity*. 2013;38(1):187–197.
90. Teijaro JR, Turner D, Pham Q, Wherry EJ, Lefrancois L, Farber DL. Cutting edge: tissue-retentive lung memory CD4 T cells mediate optimal protection to respiratory virus infection. *J Immunol*. 2011; 187(11):5510–5514.
91. Lentsch AB, Ward PA. Regulation of experimental lung inflammation. *Respir Physiol*. 2001;128(1):17–22.
92. Zeidler PC, Millecchia LM, Castranova V. Role of inducible nitric oxide synthase-derived nitric oxide in lipopolysaccharide plus interferon-gamma-induced pulmonary inflammation. *Toxicol Appl Pharmacol*. 2004;195(1):45–54.
93. Kobayashi H, et al. Antiinflammatory properties of inducible nitric oxide synthase in acute hyperoxic lung injury. *Am J Respir Cell Mol Biol*. 2001; 24(4):390–397.
94. Masopust D, Ha SJ, Vezys V, Ahmed R. Stimulation history dictates memory CD8 T cell phenotype: implications for prime-boost vaccination. *J Immunol*. 2006;177(2):831–839.
95. Kaech SM, Cui W. Transcriptional control of effector and memory CD8+ T cell differentiation. *Nat Rev Immunol*. 2012;12(11):749–761.
96. He X, et al. Mycophenolic acid-mediated suppression of human CD4+ T cells: more than mere guanine nucleotide deprivation. *Am J Transplant*. 2011; 11(3):439–449.
97. Dusting GJ, Akita K, Hickey H, Smith M, Gurevich V. Cyclosporin A and tacrolimus (FK506) suppress expression of inducible nitric oxide synthase in vitro by different mechanisms. *Br J Pharmacol*. 1999;128(2):337–344.
98. Cypel M, et al. Functional repair of human donor lungs by IL-10 gene therapy. *Sci Transl Med*. 2009; 1(4):4ra9.